

## The structural phase transition of gamma -Fe precipitates in Cu. II. Alloying effect

This article has been downloaded from IOPscience. Please scroll down to see the full text article.

1991 J. Phys.: Condens. Matter 3 7231

(<http://iopscience.iop.org/0953-8984/3/38/001>)

View [the table of contents for this issue](#), or go to the [journal homepage](#) for more

Download details:

IP Address: 171.66.16.147

The article was downloaded on 11/05/2010 at 12:33

Please note that [terms and conditions apply](#).

## The structural phase transition of $\gamma$ -Fe precipitates in Cu: II. Alloying effect

Yorihiko Tsunoda

Faculty of Science, Osaka University, Toyonaka, Osaka 560, Japan

Received 4 October 1990, in final form 29 April 1991

**Abstract.** The effect of alloying on a periodic shear wave (psw), which is observed for the low-temperature phase of  $\gamma$ -Fe precipitates in Cu, was studied by an x-ray diffraction method. The transition temperature depends on both the electronic configuration and the size of the precipitates. However, the wavelength of the psw is less affected by the alloying and is determined mainly by the size of the precipitates. Several features of the alloying effect of the psw are discussed through the data on  $\gamma$ -Fe-Co and  $\gamma$ -Fe-Cr precipitates in Cu and  $\gamma$ -Fe precipitates in a Cu-Au host.

### 1. Introduction

FCC Fe ( $\gamma$ -Fe) is stable only in a temperature range between 1185 and 1667 K under normal atmospheric conditions. However, it is well known that Fe precipitates grown in a supersaturated Cu-Fe alloy retain the  $\gamma$ -phase at room temperature. About a decade ago, Ehrhart *et al* (1980) reported that  $\gamma$ -Fe precipitates in Cu show a reduction in crystal symmetry at low temperatures. They explained the structure in the low-temperature phase as a tetragonal distortion caused by the antiferromagnetic ordering combined with a periodic arrangement of domains. The present author and a colleague (Tsunoda and Kunitomi 1988, which is paper I) recently studied this structural phase transition in more detail using an x-ray diffraction method and revealed various features of the low-temperature phase of the  $\gamma$ -Fe precipitates in Cu.

(i) In disagreement with previous workers, the atomic positions on the (001) plane for the low-temperature phase are well described as a periodic shear wave (psw) propagating along the [110] direction with the polarization vector parallel to the  $\langle 1\bar{1}0 \rangle$  direction. Along the [001] axis, the lattice contracts uniformly by about 0.17%. This is an order of magnitude smaller than that of shear deformation along the [110] direction. Thus, the lattice structure around the node of the psw is approximately orthorhombic.

(ii) The transition temperature and wavelength of the psw depend on the size of the precipitates. The larger the size, the higher is the transition temperature and the longer is the wavelength.

(iii) The amplitude of the psw behaves like an order parameter but the wavelength is independent of the temperature.

(iv) The elastic moduli  $c'$  ( $= (c_{11} - c_{12})/2$ ) and  $c_{11}$  show remarkable softening towards the transition temperature but  $c_{44}$  does not (Tsunoda and Kunitomi 1985).

(v) The precipitates with a diameter smaller than a critical value ( $d_c \approx 15$  nm) do not undergo the structural phase transition and retain a cubic structure even at the lowest temperature.

We report here the effect of alloying on this structural phase transition studied by the x-ray diffraction method. To investigate the alloying effect for this system, there are two possible choices: alloying of the solute or alloying of the host metal. The latter mainly gives us knowledge about the influence of the environment on the precipitates, while the former entails a change in the electronic configurations of the precipitates. Both of these alloying effects were studied. We chose the  $\gamma$ -Fe-Co and  $\gamma$ -Fe-Cr alloy precipitates in Cu for the former, and  $\gamma$ -Fe precipitates in Cu-Au alloy were used for the latter.

## 2. Samples and experiment

The solubilities of Co and Cr in Cu are very low and these elements are known to precipitate in Cu after an appropriate thermal treatment. Thus, we can grow  $\gamma$ -Fe-Co and  $\gamma$ -Fe-Cr alloy precipitates in the Cu host. In the same way, although the solubility of Au in  $\gamma$ -Fe is reported as 4.1 at.% at 1171 °C (Shunk 1969), it is expected to be far lower than this value at low temperatures by analogy with copper. Then we can grow  $\gamma$ -Fe precipitates in the Cu-Au alloy which has a slightly larger lattice spacing than pure Cu.

In the first place, we prepared the parent alloys  $\text{Fe}_{99.5}\text{Co}_{0.5}$ ,  $\text{Fe}_{99}\text{Co}$ ,  $\text{Fe}_{98}\text{Co}_2$ ,  $\text{Fe}_{97}\text{Cr}_3$ ,  $\text{Fe}_{92}\text{Cr}_8$  and  $\text{Cu}_{97}\text{Au}_3$  in an induction furnace. Then supersaturated alloys  $\text{Cu}(\text{Fe}, \text{Co})$ ,  $\text{Cu}(\text{Fe}, \text{Cr})$  and  $\text{Cu}_{97}\text{Au}_3(\text{Fe})$  were made in a He gas atmosphere. The solute concentration in these alloys was 2.8 at.% for all specimens. Single crystals of these alloys were grown by the Bridgman method in an  $\text{Ar}(-3 \text{ vol. \% H}_2)$  gas atmosphere. A homogenization anneal was performed at 1273 K for 24 h. After the specimens had been quenched in water, the precipitation aging was carried out.

Since the concentrations of the third elements introduced here were not so high, we assumed that the growth velocities of these alloy precipitates are approximately the same as that of pure  $\gamma$ -Fe in Cu. Accordingly, when we estimate the particle size of the precipitates, the empirical equation for pure  $\gamma$ -Fe precipitates in Cu derived by Borrelly *et al* (1975) was used.

X-ray diffraction measurements were carried out using Cu  $K\alpha_1$  radiation. To eliminate the Cu  $K\alpha_2$  component, a Ge(111) monochromator was used. The temperature was lowered to 10 K using a refrigerator unit.

## 3. Experimental data

### 3.1. $\gamma$ -Fe-Co precipitates in Cu

The structural phase transition is strongly affected by the introduction of a small amount of Co. A scattering intensity contour map observed around 400 Å at 12 K for  $\gamma$ -Fe<sub>99</sub>Co alloy (hereafter we refer to this alloy as 1 at.% Co alloy) precipitates is given in

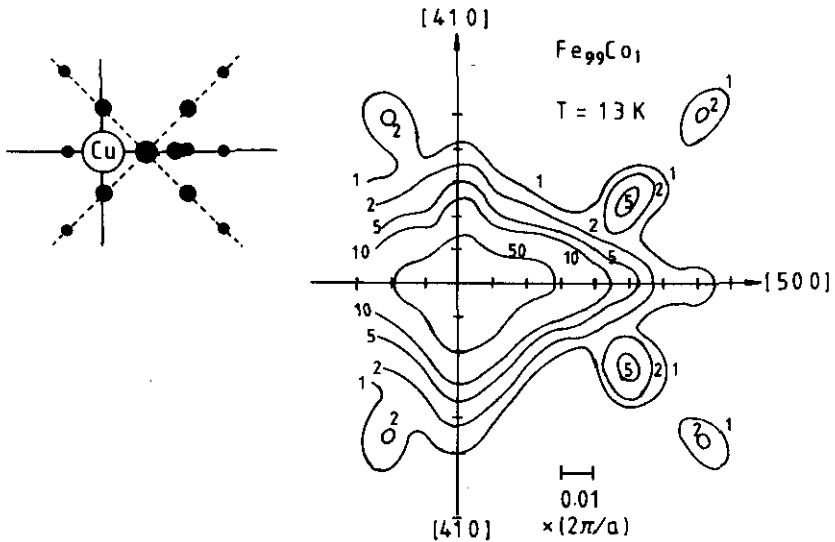


**Figure 1.** A typical intensity contour map of the low-temperature phase observed around the 400 reciprocal lattice point. The Bragg peak of the Cu host with high intensity exists at 400, the details of which are not given in this figure. The satellite peak positions are schematically illustrated on the left-hand side.

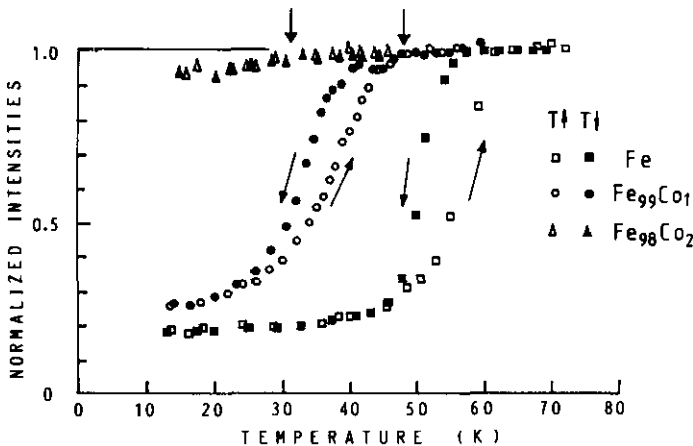


**Figure 2.** Temperature variations of the 400 Bragg peak intensities for the cubic phase of  $\gamma$ -Fe-Co precipitates.

figure 1. This is a typical diffraction pattern of the low-temperature phase with the psw and the structure analysis was published in detail in our previous paper (Tsunoda and Kunitomi 1988). From the intensity ratio of the satellites and from the satellite peak positions, respectively, we can estimate the amplitude and the wavelength of the psw. The transition temperature is determined from an abrupt decrease in the 400 Bragg peak intensity in the cubic phase. The temperature variation of the 400 Bragg peak intensity is shown in figure 2 for specimens with different Co concentrations. These data

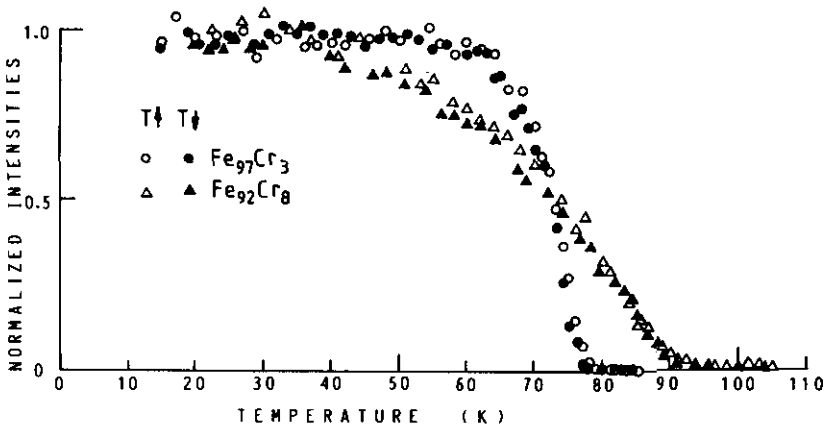


Figure 3. Temperature variations of the satellite peak intensities for the PSW in the  $\gamma$ -Fe<sub>97</sub>Cr<sub>3</sub> and  $\gamma$ -Fe<sub>92</sub>Cr<sub>8</sub> precipitates.

were obtained for precipitates with a diameter  $d \approx 50$  nm. An abrupt decrease in the intensity observed at around 35 K for the 1 at.% Co alloy is identified as the transition for PSW formation. Another type of intensity anomaly (slightly decreasing) is observed at 48 K for the 1 at.% Co alloy and at 31 K for the 2 at.% Co alloy. As pointed out in the previous paper (Tsunoda 1989a), these are the Néel temperatures for spin-density-wave (SDW) ordering. Since SDW ordering is accompanied by volume expansion, the Bragg peak position shifts slightly, resulting in a decrease in the peak intensity at the Bragg peak position of a non-magnetic phase. For the 2 at.% Co alloy, no structural phase transition for PSW formation is observed. The particle size dependence of the structural phase transition was also studied for the 0.5 at.% Co alloy specimen. The results are qualitatively the same as those for the pure  $\gamma$ -Fe precipitates in Cu. The larger the particle size, the higher is the transition temperature and the longer is the wavelength. The critical particle size of the structural phase transition varies with Co concentration. For the 1 at.% Co alloy, the critical diameter is about 50 nm. Therefore, at this Co concentration, the experimental data differ considerably from specimen to specimen. Some specimens show a structural phase transition but others do not. For the 2 at.% Co alloy, no structural phase transition is observed even for well grown precipitates.

### 3.2. $\gamma$ -Fe-Cr precipitates in Cu

Two alloy specimens containing 3 and 8 at.% Cr, were studied. A special feature of the precipitates in these alloys is that the lattice spacing expands by alloying with Cr. The lattice spacing at room temperature is larger than that of pure  $\gamma$ -Fe precipitates in Cu by about 0.01% for each 1 at.% Cr. Both of the specimens show a structural phase transition at low temperatures. The transition temperature considerably increases by alloying with Cr. The temperature variation of the satellite peak intensities for the alloy precipitates observed in the low-temperature phase around 400 are shown in figure 3. For the 8 at.% Cr alloy the behaviour of the phase transition differs markedly. The phase transition behaves in an almost second-order manner. Although the transition temperature is the highest of all the specimens studied, the zeroth-order peak has a strong

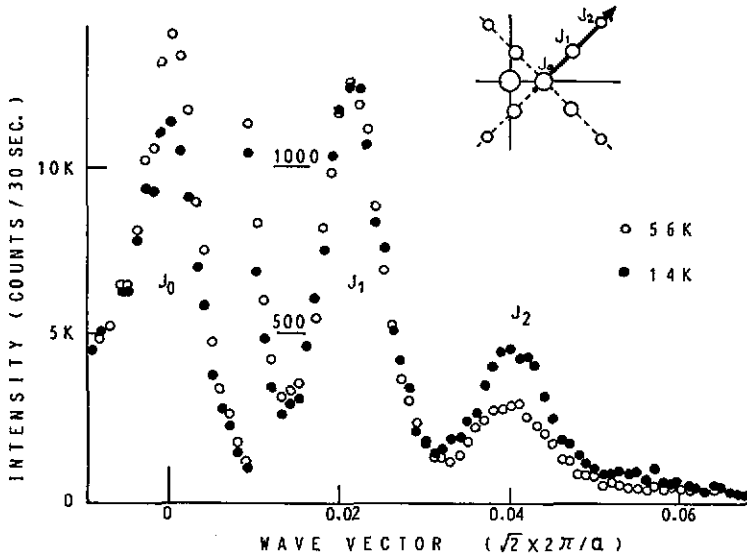


Figure 4. Diffraction patterns of the satellite peaks observed at different temperatures by scanning along the  $[110]$  direction around 400. The relative peak intensities change with temperature but there is no change in the peak position.

intensity and the second-order satellite peaks are very weak, indicating that the amplitude of the PSW is very small. Diffraction patterns of the satellite peaks for the 3 at. % Cr alloy observed by scanning along the  $[110]$  direction around 400 are compared for different temperatures in figure 4. The intensity ratio of the satellite peaks varies with temperature, but there is no change in the satellite peak positions, i.e. the amplitude of the PSW varies with temperature, but the wavelength is independent of temperature. This is a common feature of the PSW for all other specimens.

### 3.3. $\gamma$ -Fe precipitates in $\text{Cu}_{97}\text{Au}_3$

The lattice spacing of  $\text{Cu}_{97}\text{Au}_3$  is larger than that of pure Cu by about 0.5% (Finkler *et al* 1987). If the lattice spacing of  $\gamma$ -Fe precipitates in  $\text{Cu}_{97}\text{Au}_3$  alloy retains the same value as that obtained previously in pure Cu, then the 400 Bragg peak of  $\gamma$ -Fe precipitates should appear at 4.049 00 in the reciprocal lattice frame of  $\text{Cu}_{97}\text{Au}_3$ . However, the observed peak position is 4.041 00 at room temperature, indicating that the lattice spacing of  $\gamma$ -Fe precipitates in  $\text{Cu}_{97}\text{Au}_3$  is slightly larger than that in Cu (about 0.2%). As shown below, this is not due to the inclusion of Au in  $\gamma$ -Fe precipitates. Thus, we can study the effect of lattice expansion on the structural phase transition in  $\gamma$ -Fe precipitates. Temperature variations of the 400 Bragg peak intensities for the specimen with various aging periods are shown in figure 5. The transition temperature depends on the particle size of the precipitates as observed for  $\gamma$ -Fe in Cu. However, the transition temperature of  $\gamma$ -Fe precipitates in Cu-Au is higher than that of  $\gamma$ -Fe in Cu with the same particle size. The wavelength of the PSW becomes longer on increase in the particle size. This is also a common feature of the PSW in  $\gamma$ -Fe and  $\gamma$ -Fe alloy precipitates in Cu.

For the well aged specimens, the  $\gamma$ -Fe precipitates become non-coherent, although some of the precipitates transform to a BCC phase during aging. This state still retains

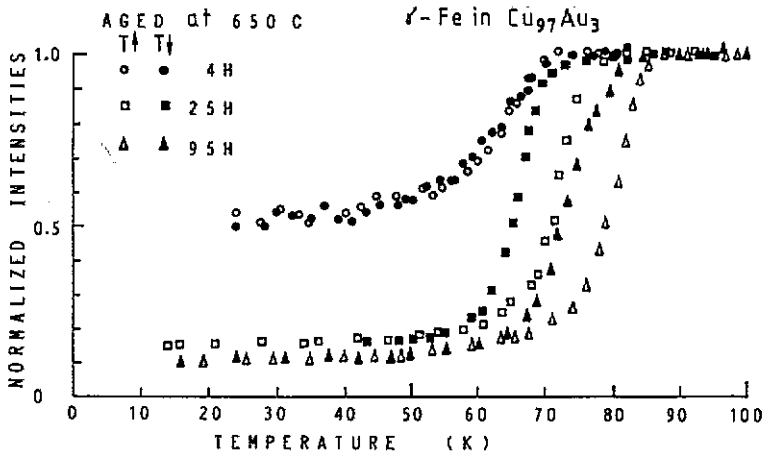


Figure 5. Temperature variations of the 400 Bragg peak of  $\gamma$ -Fe precipitates in  $\text{Cu}_{97}\text{Au}_3$  alloy in the cubic phase are given as a function of the aging period.

Table 1. Properties of the PSW for various  $\gamma$ -Fe alloy precipitates with the same particle size. All specimens except for  $\gamma$ -Fe in Cu were aged at 923 K for 70 h.  $\gamma$ -Fe was aged at 973 K for 14 h;  $d \approx 56$  nm.

Host	Precipitate	Wavevector $\sqrt{2} \times 2\pi/a$	Wavelength (nm)	Amplitude (nm)	Transition temperature (K)
Cu	Fe	0.0235	10.76	0.043	54 ( $T \downarrow$ ), 60 ( $T \uparrow$ )
$\text{Cu}_{97}\text{Au}_3$	Fe	0.023( $\pm 0.002$ )	11.0( $\pm 0.9$ )	0.047( $\pm 0.002$ )	80 ( $T \downarrow$ ), 82 ( $T \uparrow$ )
Cu	$\text{Fe}_{99}\text{Co}_1$	0.024( $\pm 0.001$ )	10.6( $\pm 0.4$ )	0.036( $\pm 0.002$ )	38 ( $T \downarrow$ ), 42 ( $T \uparrow$ )
Cu	$\text{Fe}_{97}\text{Cr}_3$	0.021( $\pm 0.002$ )	12.0( $\pm 1.0$ )	0.041( $\pm 0.002$ )	76 ( $T \downarrow$ ), 77 ( $T \uparrow$ )
Cu	$\text{Fe}_{92}\text{Cr}_8$	0.020( $\pm 0.002$ )	12.6( $\pm 1.1$ )	0.021( $\pm 0.003$ )	90 ( $\pm 2$ )

crystal axes parallel to those of the matrix, but the lattice spacing contracts markedly and many dislocations appear at the interface between the precipitates and the matrix (Easterling and Miekko-Oja 1967). The observed lattice spacing of non-coherent  $\gamma$ -Fe precipitates in  $\text{Cu}_{97}\text{Au}_3$  is just the same as that in the pure Cu matrix. This verifies that  $\gamma$ -Fe precipitates in the  $\text{Cu}_{97}\text{Au}_3$  alloy do not include an appreciable amount of Au.

#### 4. Discussion

Since the structural phase transition depends on the size of the precipitates, the effect of alloying should be studied for the precipitates with the same particle size. The properties of the PSW in these alloys are compared in table 1 for precipitates with the same particle size (about 50 nm). Although the transition temperatures for these alloy precipitates vary considerably with the alloying element and composition, the wavelength of the PSW is almost constant for all specimens. As we reported previously (Tsunoda 1989a), the incommensurate SDW observed in the cubic  $\gamma$ -Fe-Co precipitates behaves in a different way. The wavelength and Néel temperature of the SDW are

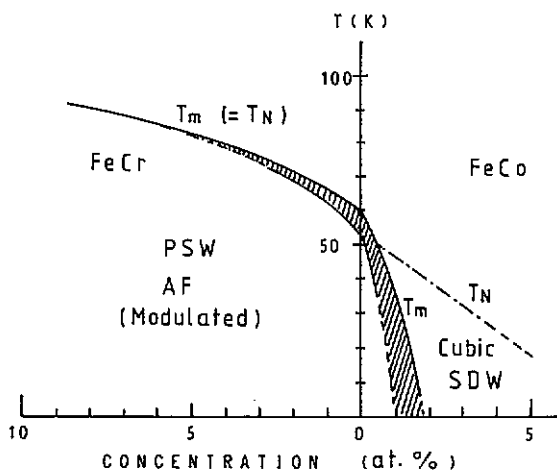


Figure 6. Transition temperatures of the  $\gamma$ -Fe-Co and  $\gamma$ -Fe-Cr alloy precipitates in Cu. The Néel temperatures determined by neutron diffraction are also given.

independent of the particle size for large precipitates but depend on the Co concentration. This is a decisively different point between the PSW and the SDW. The stabilization of the SDW is a purely electronic problem in precipitates (at least for large precipitates). However, the PSW formation is not determined only from the electronic configuration inside the precipitates. As shown for  $\gamma$ -Fe precipitates (Tsunoda and Kunitomi 1988), the strain energy stored at the interface region plays an important role in determining the PSW formation. Thus the present study on the alloying effect of precipitates leads to the conclusions that the transition temperature  $T_m$  of the PSW formation (the stability of the low-temperature phase) depends on both the electronic configuration and the interfacial strain energy. On the other hand, the wavelength of the PSW is less affected by the alloying and seems to be determined only by the particle size. The amplitude of the PSW is rather complicated. It behaves like an order parameter for the temperature variation but, since the amplitude correlates with the wavelength, it is not a simple function of these factors, especially for a PSW with a long wavelength. These are distinctive features of the PSW observed in  $\gamma$ -Fe and  $\gamma$ -Fe alloy precipitates in Cu.

Since the structural phase transition takes place at the onset of antiferromagnetic ordering for the  $\gamma$ -Fe precipitates, it is important to clarify the relation with the magnetism in order to investigate the cause of this structural phase transition. One of the purposes of studying the alloying effect is to solve this problem.

In figure 6, the phase diagram of  $\gamma$ -Fe-Co and  $\gamma$ -Fe-Cr alloy precipitates determined by the present measurements is given together with the Néel temperature; some of these data were reported previously (Tsunoda 1989a). Figure 6 shows the observed values for a particle size of 50 nm. The structural phase transition is strongly suppressed by the introduction of Co. The Néel temperature also decreases with increasing Co concentration but is less affected by the alloying of Co. The  $T_m$  and  $T_N$  lines separate at around 0.7 at. % Co and the  $T_m$  line disappears at 2 at. % Co. However, the extrapolated  $T_N$  line disappears at around 8 at. % Co. This implies that the structural phase transition is not caused by the simple magnetostriction due to magnetic ordering. In fact, as shown in the previous paper (Tsunoda 1989a), the magnetic structure of  $\gamma$ -Fe-Co precipitates



in the cubic phase is an incommensurate SDW state with the modulation vector along the [010] direction and with a wavelength of about ten times the lattice spacing. Small  $\gamma$ -Fe precipitates, for which the structural phase transition is suppressed, also have a SDW structure. The symmetry of this magnetic structure is different from that of the local lattice structure of the PSW. Rather the spin structure on the PSW seems to be affected by the structural phase transition (Jo 1989). It reflects the lattice symmetry of the PSW and has the same period and propagation direction as the PSW (Tsunoda *et al* 1987). An antiferromagnetic structure on the FCC lattice has some contradictory coupling. Since the structural phase transition reduces the lattice symmetry, the antiferromagnetic ordering is stabilized on PSW formation and  $T_N$  increases up to  $T_m$ . This is the reason why the Néel temperature of  $\gamma$ -Fe precipitates depends on the particle size (Keune *et al* 1989) although the Néel temperature of the SDW in the cubic  $\gamma$ -Fe-Co precipitates is independent of the particle size as long as the precipitates are of reasonable size (Tsunoda 1990). Thus, the structural phase transition and magnetic ordering seem to be different and it is hard to prove that the PSW is induced by the magnetic ordering through magnetoelastic coupling.

A periodic structure having similar properties to the PSW is known as microtwins and these are widely observed by electron microscopy after martensitic transformation. In the present case, however, the lattice displacement varies continuously in space and no lattice imperfections such as dislocations are involved across the modulated lattice. Thus, the PSW is a new type of incommensurate lattice wave. The existence of this type of periodic lattice wave has been predicted theoretically by several workers as a pre-martensitic modulated phase (Olson and Cohen 1982, Barsch and Krumhansl 1984, Barsch *et al* 1987, Suzuki *et al* 1987). The possibility of a pre-martensitic phase of the FCC-to-BCC martensitic transformation in Fe was discussed in our previous paper (Tsunoda 1989b) and we shall not repeat the discussion here.

The introduction of Co suppresses the structural phase transition markedly but the alloying of Cr raises the transition temperature. The origin of this behaviour is, of course, considered to be that the electronic configuration of the Co alloy precipitates stabilizes the FCC structure and it becomes unstable for alloying with Cr. However, another factor must also be considered in the present case. Alloying with Co leads to a slight decrease in the lattice spacing of the  $\gamma$ -Fe-Co precipitates. Since the strain at the interface plays a very important role in PSW formation, the increase in the lattice spacing mismatch due to the alloying with Co strongly acts to suppress the structural phase transition. On the other hand, the introduction of Cr decreases the mismatch of the lattice spacings, resulting in an increase in the transition temperature.

The lattice spacing of  $\gamma$ -Fe precipitates in  $\text{Cu}_{97}\text{Au}_3$  alloy is slightly larger than that of the precipitates in pure Cu. Thus, we can study the effect of a negative pressure on this system. The experimental data show an increase in the transition temperature. Generally speaking, lattice expansion leads to lattice softening, resulting in an increase in the transition temperature. In the present case, however, the situation may not be simple because we have to consider the effect due to the increase in the lattice spacing mismatch between the  $\gamma$ -Fe precipitates and the Cu-Au host matrix.

## References

- Barsch G R and Krumhansl J A 1984 *Phys. Rev. Lett.* **53** 1069–72  
Barsch G, Krumhansl J A, Tanner L E and Wuttig M 1987 *Scr. Metall.* **21** 1257–62  
Borrelly R, Pelletier J M and Pernoux E 1975 *Scr. Metall.* **9** 747–52

- Easterling K E and Miekko-Oja H M 1967 *Acta Metall.* **15** 1133-41
- Ehrhart P, Schonfeld B, Ertwig H H and Pepperhoff W 1980 *J. Magn. Magn. Mater.* **22** 79-85
- Finkler D K-H, Maurer A E, Campbell S J, Heck T and Gonser U 1987 *Physica B* **145** 335-41
- Jo T 1989 *J. Phys.: Condens. Matter* **1** 7971-5
- Keune W, Ezawa T, Macedo W, Glos U, Schlets K P and Kirschbaum U 1989 *Physica B* **161** 269-75
- Olson G B and Cohen M 1982 *J. Physique* **43** C4 75-88
- Shunk F A 1969 *Constitution of Binary Alloys, Second Supplement* (New York: McGraw-Hill) p 70
- Suzuki T, Yuan Lei C Y and Wuttig M 1987 *Proc. Int. Conf. on Martensitic Transformations (Nara 1986)* (Sendai: Japan Institute of Metals) pp 55-60
- Tsunoda Y 1989a *J. Phys.: Condens. Matter* **1** 10 427-38
- 1989b *J. Phys. Soc. Japan* **58** 1648-54
- Tsunoda Y 1990 *Prog. Theor. Phys. Suppl.* **101** 133-8
- Tsunoda Y and Kunitomi N 1985 *Solid State Commun.* **54** 547-9
- 1988 *J. Phys. F: Met. Phys.* **18** 1405-20
- Tsunoda Y, Kunitomi N and Nicklow R M 1987 *J. Phys. F: Met. Phys.* **17** 2447-58